Cold-formed steel Z-section columns affected by phenomena of interaction between local-plate and distortional buckling modes

C. Barreta

Department of Civil Engineering, IST, Technical University of Lisbon

Abstract

One presents and discuss the results of a study on the behavior of post-buckling in elastic and elastic-plastic, steel cold formed Z-section affected by phenomena of interaction between local-plate/distortional buckling modes. All geometric and physically nonlinear analysis are carried out by finite element method using the program ABAQUS and adopting shell elements to discretize the columns. The analyzed columns (i) exhibit extreme articulated sections (locally and globally) and are warp free, (ii) have cross sections with dimensions that provide similar local-plate/distortional stress values (iii) contains geometric imperfections with various configurations (linear combinations of local-plate/distortional modes) and a common amplitude. The numerical results consist of (i) elastic and elastic-plastic post-buckling trajectories, (ii) curves that describe how the deformed configuration of the column evolves along the elastic trajectories and (iii) figures showing the plastic deformation evolution and the elastic-plastic columns collapse mode characteristics.

Keywords: Cold formed steel Z-section columns; Local-plate and distortional buckling; Mode interaction; Elastic and elastic-plastic post-buckling; Finite element method

1. Introduction

Most cold-formed steel members display very slender thin-walled open cross-sections, a feature making them highly susceptible to local instability phenomena, namely (i) *local-plate* and (ii) *distortional* buckling. Moreover, since several commonly used members exhibit cross-section geometries (shape and/or dimensions) associated with rather similar local-plate and distortional bifurcation stresses, their overall structural behaviours are likely to be affected by the occurrence of mode interaction phenomena involving the above two (local) buckling modes.

In order to assess the overall structural behaviour of thin walled members affected by local buckling effects, steel designers are currently faced with two options: either (i) resort to highly complex and computer intensive numerical methods (an approach still prohibitive for routine applications), or (ii) take those effects into account indirectly, through their incorporation into member global analysis (e.g., FEM analysis adopting non-linear beam finite elements). The latter strategy can only be rational and fully efficient provided that the knowledge concerning the member local post-buckling behaviour is solid/deep enough to enable the development of reliable and physically based models. For instance, this is the case of (i) the well-known "plate effective width" concept, accounting for local-plate effects, or (ii) the recently developed and very potent "direct strength method", which can handle both local-plate and distortional effects and takes into consideration the whole cross-section behaviour (e.g., [1]). However, as far as the local-plate/distortional bucking mode interaction effects are concerned, only a limited number of (recent) studies have yet been reports – e.g. works by Schafer and Pekoz [2], Ungureanu and Dubina [3], Yang and Hancock [4], Silvestre e Camotim [5] or Dinis et al. [6].

The aim of this paper is to present and discuss the results of a shell finite element

numerical investigation dealing with the influence of local-plate/distortional buckling mode interaction on the elastic and elastic-plastic post-buckling behaviour and strength of cold-formed steel Z-section columns (*i.e.*, uniformly compressed members) – moreover, the nature of the columns elastic-plastic failure mechanism is also addressed. The columns analysed exhibit (i) the cross-section dimensions indicated in Figure 1, ensuring *equal* local-plate and distortional critical stresses, (ii) the material constants also given in Figure 1, (iii) several yield stress values and (iv) extreme articulated sections (locally and globally) and are warp free. Since the main goal of this work is to assess the local-plate/distortional mode interaction effects, one must determine the post-buckling behaviours of columns containing initial imperfections exhibiting a wide variety of critical-mode shapes and sharing the same combined amplitude. After addressing a number of relevant finite modelling issues, one reports a set of numerical results that were obtained by means of finite element analysis performed in the code ABAQUS [7], and adopting fine meshes of 4-node shell elements to discretise de columns. These results consist of (i) elastic and elastic-plastic non-linear post-buckling equilibrium paths, (ii) curves and figures that describes how the columns deformed configuration (expressed as a linear combination of its local-plate and distortional components) evolves along the elastic post-buckling equilibrium paths and (iii) figures making it possible to visualize (iii_1) the evolution of the elastic-plastic column deformed configurations, (iii_2) the growth of the plastic strains and (iii_3) the failure mechanisms exhibited by several elastic-plastic columns.

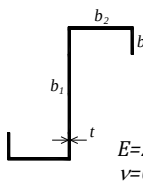

b_1 [mm]	b_2 [mm]	b_3 [mm]	t [mm]
100	60	10	1,5

Figure 1. Z-section geometry, cross section dimensions and elastic constants.

2. Finite element modelling

This section deals with the use of finite element code ABAQUS [7] to perform the column post-buckling analysis. In particular one addresses issues related to (i) the column discretisation, (ii) the modelling of the column support conditions, applied loads and material behaviour, (iii) the incorporation of the initial geometrical imperfections and (iv) the numerical techniques employed to solve either the linear stability eigenvalue problem or the system of non-linear equations providing the post-buckling equilibrium paths.

2.1. Member discretisation

In order to analyse both the local and global behaviours of a given thin-walled member, one must adopt a two-dimensional model (*i.e.*, to discretise its mid-surface), a task that can be adequately performed by means of isoparametric shell finite elements. Previous studies by the first two authors [8] have shown that this task that can be adequately performed by means of S4 elements (ABAQUS notation – 4-node isoparametric fully integrated shell element allowing for a transverse shear deformation[1]).

In order to determine the level of mesh refinement required to obtain accurate results, while keeping the computational effort involved within reasonable bounds, a preliminary investigation was carried out. For the particular case of the Z-section columns dealt with in this work, it was found that it suffices to discretise the cross-section by means of (i) 28 FEs (10 in the web, 8 in each flange and 1 in each stiffener) – this roughly corresponds to adopting FEs with a 10mm width. Concerning the longitudinal direction, the number of FEs considered should ensure that an element length/width ratio comprised between 1 and 2 [8].

2.2. End support conditions

In order to enable meaningful comparisons between (i) numerical results yielded by different methods or (ii) numerical and experimental results, its essential to make sure that the member end support conditions are adequately modelled. First of

[1] It is worth that the use of S4R (reduced integration) elements, extensively employed, underestimates the column distortional post-critical strength. This rather surprising feature stems from the fact that the reduced integration procedure (intended to preclude the occurrence of shear locking) cannot fully capture the columns shear stiffness due to the non-linearity of the wall warping displacements [8,9].

all, it is necessary to make a clear distinction between global and local support conditions: while the former deal with the end section rigid-body translator movements (one axial and two transversal) and rotations (one torsional and two flexural), the latter involve the displacements of the wall transverse edges, with respect to the end section location after its rigid-body motion. Among the local conditions, one still distinguishes between the ones concerning the end section (i) warping (axial displacements) and (ii) in-plane deformation (transversal membrane/flexural displacements and derives with respect to the longitudinal axis). Next, one lists and describes a number end support conditions that are more or less frequently (i) modelled in numerical analysis and/or (ii) physically executed in experimental investigations [10]:

(i) *Free end* section. All the global and local displacements/rotations are free. This is the condition implemented in the overwhelming majority of columns experimental tests.

(ii) *Fixed end* section. All the global and local displacements/rotations are prevented.

(iii) *Simply supported* end section. The following displacements/rotations are prevented: (iii_2) transversal membrane and flexural displacements (local).

(iv) *Locally fixed and globally simply supported* end section. Only the global transversal translator motion and torsional rotation are free.

(v) *Locally pinned and globally fixed* end section. This condition, which may be viewed as "almost fixed", differs from the fixed one (see item (ii)) in the fact that flexural rotations may occur at the wall transverse edges.

As mentioned above, all the columns extreme sections were considered as simply supported, meaning that these sections are pinned and can warp freely. The support conditions adopted here were modelled (i) preventing transverse displacements and (ii) allowing the axial displacement and bending rotations of all nodes in the extreme sections. To avoid numerical problems related to rigid-body motions, there where also prevented (i) torsional rotations in extreme sections and (ii) the axial displacement of the node located on half height of the web of the mid-span section of the column.

2.3. Loading

Equal uniform compressive distributed loads were applied at both end-sections. This distributed load p is the load parameter and its reference value is t N/mm (t is the column wall thickness), which corresponds to a 1MPa uniform stress distribution. Thus, the load parameter value yielded by ABAQUS provides the average stress acting on the column (MPa) – the applied load can be obtained by merely multiplying this value by the cross sectional area.

2.4. Initial geometrical imperfections

Initial geometric imperfections can be incorporated in a member post-buckling analysis performed in the code ABAQUS either (i) manually, by directly inputting an arbitrary initial configuration, or (ii) automatically, trough the *a priori* definition or a linear combination of buckling mode shapes, obtained from a preliminary stability analysis. In this work, the column initial geometrical imperfections were included automatically, as different linear combinations of the following (critical) buckling mode shapes (see Figure 2(b)). The linear combinations were incorporated into the column initial geometry by means of a specific ABAQUS command.

2.5. Material Behaviour modelling

The column (steel) material behaviour was always assumed to be homogeneous and isotropic and two constitutive laws were considered to model it, namely (i) a linear-elastic/perfectly-plastic law (strain hardening was neglected). The linear elastic behaviour is fully characterized by the values of Young's modulus E and Poisson's ratio ν. As for the elastic-plastic behaviour, it is described by means of the well-known Prandtl-Reuss model, combining Von Mises' yield criterion with an associated flow rule. These models are readily available in the ABAQUS material behaviour library and their implementation just involves providing the steel elastic constants and yield stress f_y.

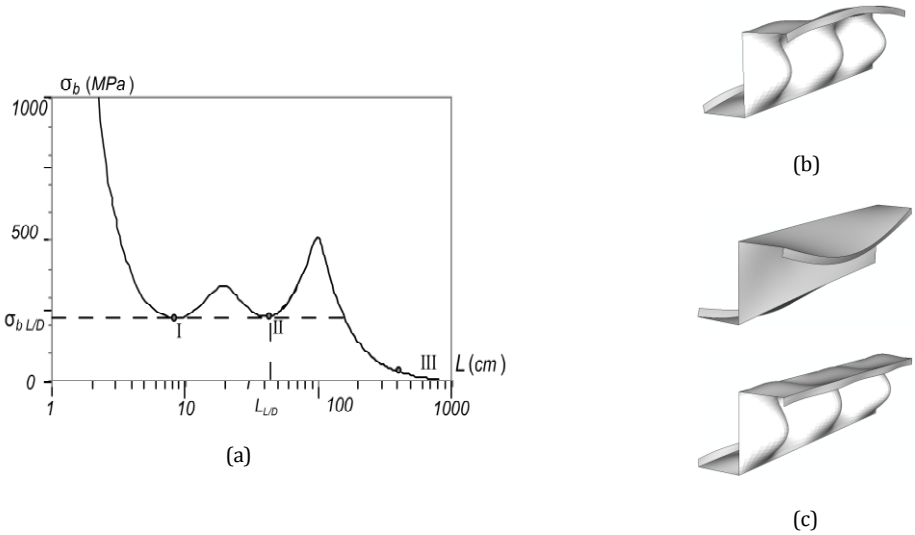

Figure 2. Buckling results: (a) σ_{cr} vs. L curve (b) critical-mode shape "combine" L/D (L=403 mm) and (c) pure distortional and local-plate modes.

2.6. Numerical solution techniques

The performance of a linear stability analysis requires solving an eigenvalue problem, defined by the column (discretised) elastic stiffness and geometric matrices – in ABAQUS, the "sub-space interaction method " is used to obtain this solution.

As for the non-linear (post-buckling) equilibrium paths, relating the applied stress value to a suitably chosen column displacement, they are determined by means of a numerical incremental-interactive technique, using Newton-Raphson's method. Since both the column elastic local-plate and distortional post-buckling behaviours are stable, all the elastic analysis were performed using load (stress) control. Conversely, as the column elastic-plastic behaviour exhibits a limit point (ultimate strength value), the elastic-plastic analysis had to be performed employing Riks's arc-length control strategy, which is automatically adopted by ABAQUS and implemented with a pre-defined "calibration" – increment and tolerance parameters.

3. Buckling behaviour

The curve depicted in Figure 2(a) concern an extreme articulated Z-section column and provide the variation of the critical stress σ_{cr} with the column length L (in logarithmic scale). Figure 2(b) on the other hand, displays the FEM-based critical buckling mode shape that belongs to a 403 mm length column with the cross-section presented previously and that shows a not unique configuration – it is as arbitrary combination of a 5-wave local-plate mode and a 1-wave distortional mode, both of which are associated with the same critical stress value (Figure 2(c)). These two buckling mode shapes were obtained through preliminary linear stability analysis, which should be based on a finite element mesh identical to the one adopted to perform the post-buckling analysis, and their linear combinations were incorporated into the column initial geometry by means of a specific ABAQUS command.

4. Post-buckling behaviour under mode interaction

In this section, one investigates the elastic and elastic-plastic post-buckling behaviour of extreme articulated Z-section columns with (i)the cross section geometry presented in Figure 1 and (ii) a length L=403mm. As shown, these columns bifurcate (elastically) for σ_{cr}=221MPa in modes that exhibit arbitrary combinations of (i) 5 local-plate waves and (ii) three distortional waves. This means that strong interaction between these two buckling

mode shapes is to be expected. Note also that the elastic-plastic columns analysed display different yield stresses, corresponding to the yield stress values f_y=355, 460, 550 MPa (f_y=∞ for elastic columns).

4.1. Initial geometrical imperfections

The shape of the initial geometrical imperfections always plays a crucial role in mode interaction investigations, since its choice may alter considerably the post-buckling behaviour and strength of the structural system under consideration. Indeed, the usual approach of including critical-mode imperfections ceases to be well defined, due to the presence of two "competing" buckling modes that may be combined arbitrarily. Thus, in order to obtain column equilibrium paths that (i) cover the whole imperfections shape range and (ii) can be meaningfully compared, the following approach was adopted:

(i) To determine the "pure" critical buckling mode shapes (represented in Figure 2(c)) with unit mid-span (i_1) mid-web flexural displacement (local-plate – w_L=1) and (i_2) flange-lip corner vertical displacement (distortional – v_D=1) [2]. Then, a given combined imperfection shape is obtained as a linear combination of the pure modes, with coefficients $C_{L,0}$ and $C_{D,0}$. Note that, in general, both buckling modes will contribute to w_0 and v_0, i.e., one has

$$w_0=C_{D,0}w_{D,0}+C_{L,0}w_{L,0} \quad (1)$$

$$v_0=C_{D,0}v_{D,0}+C_{L,0}v_{L,0} \quad (2)$$

where $w_{L,0}$, $v_{L,0}$, $w_{D,0}$ e $v_{D,0}$ are those described displacements for each buckling mode and $C_{L,0}$ and $C_{D,0}$ stand for the aforementioned contributions.

(ii) All initial imperfections share the same combined magnitude, which equal to 10% of the wall thickness, t. In order to achieve this, one begins by normalizing the pure modes in such a way that $w_{L,0}=0,1t$ and $v_{D,0}=0,1t$ (in this particular case, $0,1t$=0,15mm). Then, one ensures the above combined amplitude by simply enforcing the condition

$$(C_{L,0})^2 + (C_{D,0})^2 = 1 \quad (3)$$

(iii) A better visualization and "feel" of the initial imperfection shape can be obtained by considering the 1,0 radius circle represented in the $C_{L,0}$- $C_{D,0}$ plane as shown in Figure 3(b): each "acceptable" imperfection shapes lies on this circle and corresponds to an angle θ, measured counter clockwise from the horizontal ($C_{D,0}$) axis and defining the ratio $C_{D,0}/C_{L,0}$ ($C_{D,0}=cos\theta$ and $C_{L,0}=sin\theta$). Figure 3(a) shows the FEM-based initial imperfection shapes associated with $\theta=0°$, $180°$ (pure distortional shape) and $\theta=90°$, $270°$ (pure local-plate shape). Finally note that (iii_1) (by rotating the deformed picture, is possible to demonstrate that both shapes are equal) and (iii_2) $\theta=90°$ and $\theta=270°$ have similar deformed shape (by the same reason). Which by the section symmetry is plausible to confirm that the columns behaviour are the same and by that one will only present the $0°\leq\theta\leq90°$ results.

(iv) The initial imperfections considered in this work are associated with 15° angle intervals.

4.2. Elastic interactive behaviour

First, one addresses the influence of the local-plate/distortional mode interaction in the elastic post-buckling behaviour of the previous chosen column (Figure 1), L=403mm. For this column there were considered 24 distinct initial imperfections, which basically means that 24 different columns were analysed.

The post-buckling equilibrium paths displayed in Figure 4(a) and 4(c) (P/P_{cr} vs. v/t) and Figure 4(b) and 4(d) (P/P_{cr} vs. w/t) correspond to columns containing pure distortional and pure local-plate initial geometrical imperfections. After observing these figures, the following conclusions can be drawn:

(i) On a post-buckling advanced stadium, all four columns display a combined deformed shape, with notorious presence of both distortional and local-plate evidence – both displacements v and w non-null.

[2] Note that, in order to be able to "separate" the local-plate and distortional modes, it was necessary to perform FEM buckling analysis in columns with slightly altered wall thickness values.

(ii) The columns θ=90°, 270° are likely to be more resistant than θ=0°, 180°, which means those columns with initial local-plate imperfections support a higher post-buckling load.

(iii) The distortional mode is more important on the final configuration and show bigger displacements, but the presence of local-plate displacements reveals the interaction mode.

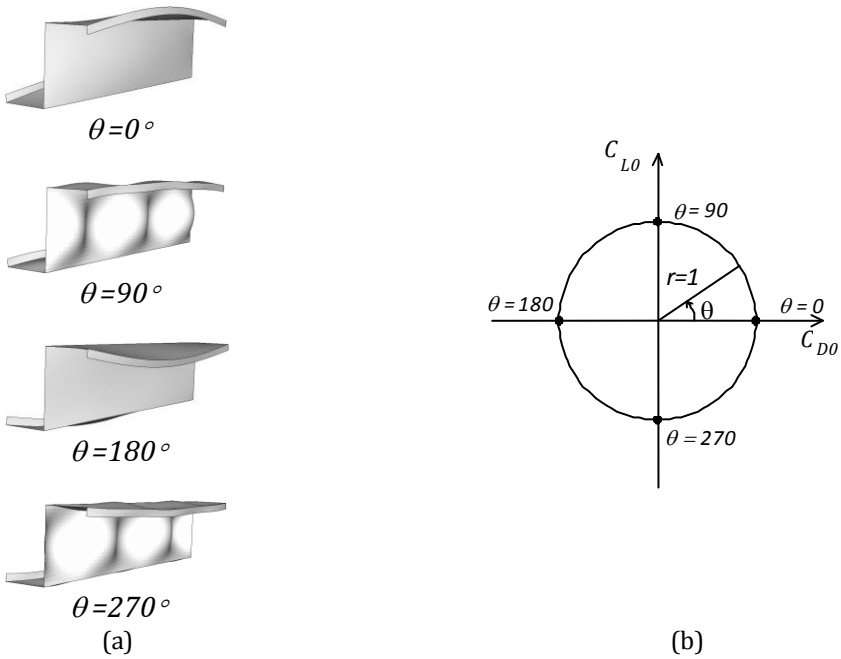

Figure 3. (a) Four FEM-based imperfection shapes (θ =0°, 90°, 180°, 270°) and (b) initial geometrical imperfection in the plane $C_{L,0}$- $C_{D,0}$.

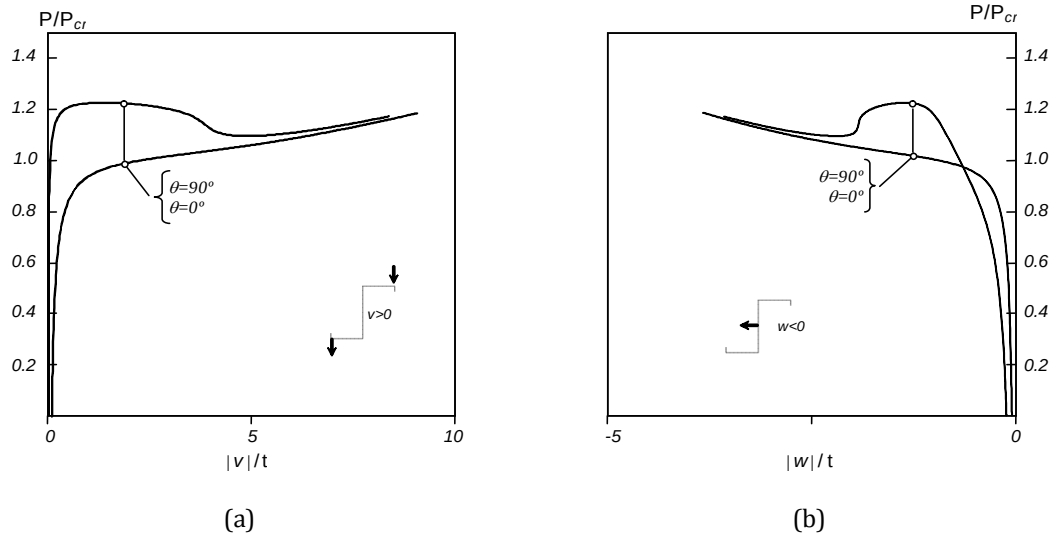

Figure 4. Post-buckling behaviour of Z-section column with pure distortional and local-plate initial imperfections: (a) P/P_{cr} vs. v/t paths; (b) P/P_{cr} vs. w/t paths

Figure 5 shows the upper portions of several additional column post-buckling equilibrium paths P/P_{cr} *vs.* v/t, which correspond to intermediate θ values between $0° \leq \theta \leq 90°$. In order to provide a better understanding of the overall results, these figures also include the "limit" curves $\theta = 0°$, $90°$, which were already shown in previous figures. The observation of this set of equilibrium paths leads to following conclusions:

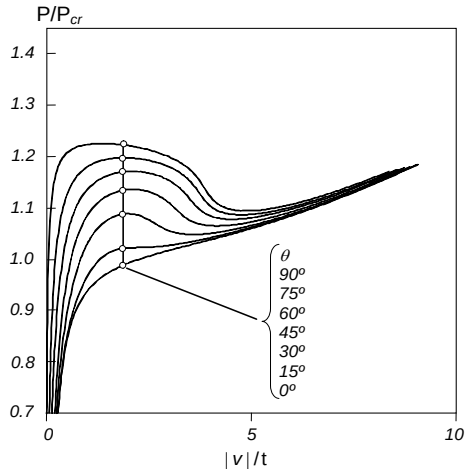

Figure 5. Elastic post-buckling equilibrium paths P/P_{cr} vs. v/t, $0° \leq \theta \leq 90°$.

(i) All equilibrium paths merge to the one concerning the pure initial distortional deformations.

(ii) All the non-pure imperfection columns are more resistant than the one that have pure distortional imperfections.

(iii) Some of the curves present "snap-trough" phenomena due to the necessity of changing their original path so that they can converge to the pure initial distortional imperfections curves[3].

Finally, Figure 6 shows the evolution, along the several equilibrium paths considered, of a "mode-coupling ratio" defined as $C_{D,0}/C_{L,0}$ and relating the amplitudes of the local-plate and distortional components of the column deformed configuration.

These amplitudes are obtained (i) on the basis of the maximum values of the mid-web flexural displacement (w_{max}) and flange-lip corner displacement (v_{max}), both occurring at mid-span, and (ii) adopting the following assumptions and methodology:

(i) The column deformed shape configuration can be exactly expressed as linear combination of 5-wave local-plate and 1-wave distortional buckling mode shapes.

(ii) The deformed shape configuration distortional component is the sole responsible for v_{max}. This is not 100% true, as the local-plate mode also has a (very small) contribution for the v value.

(iii) The value of w_{max} comprises two parts, one due to the local-plate component ($w_{max,L}$) and the other to its distortional counterpart ($w_{max,D}$). The second one can be readily determined if one takes into account that the distortional buckling mode shape is characterized by the ratio w=0,619v.

(iv) In view of the above assumptions, the values of C_D and C_L are given by the expressions $C_D = v_{max}/v_0$ and $C_L = (w_{max} - 0{,}619 v_{max})/w_0$, respectively.

[3] These phenomena occur by removal of excess of one of the buckling modes in that column.

The C_L/C_D curves shown in Figure 6 provide the following information about the column local-plate/distortional mode interaction behaviour:

(i) Initially, all curves are 1,0 apart from the origin (see detail) and exhibit a variable slope, which depends on the shape of the initial imperfection.

(ii) The various C_L/C_D curves converge to two practically straight lines with slightly different slopes (ii$_1$) $\Delta C_L \approx 0{,}050\ \Delta C_D + 0{,}200$ ($0° \leq \theta \leq 90°$ and $270° \leq \theta \leq 360°$) and (ii$_2$) $\Delta C_L \approx 0{,}167\ \Delta C_D + 0{,}583$ ($90° < \theta \leq 270°$). It seems reasonable to assume that these straight lines define the column, predominantly distortional, "coupled buckling modes".

(iii) The two "coupled mode" straight lines correspond to C_L and C_D values with the signs, coupled – one with both C_L and C_D positive signs and the other with negative signs. This shows that the corresponding column deformed configurations combine local-plate and distortional mid-web flexural displacements favouring each other at the mid-span region.

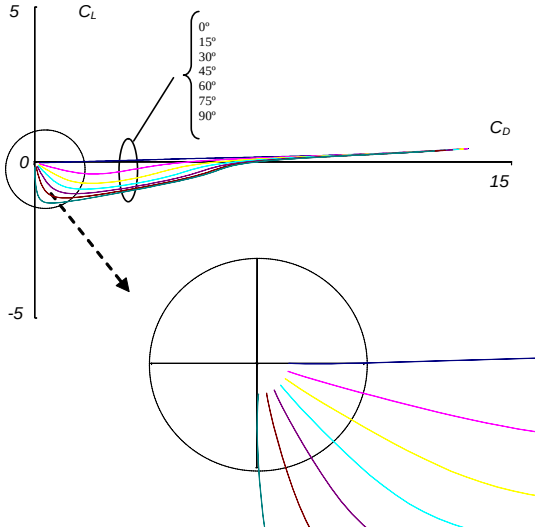

Figure 6. Evolution of the mode coupling ratio C_L/C_D along the equilibrium paths.

4.3. Elastic-plastic interactive behaviour

In this section, one addresses the influence of the local-plate/distortional mode interaction in the elastic-plastic post-buckling behaviour of Z-section columns (i) containing seven initial imperfection shapes ($0° \leq \theta \leq 90°$) and (ii) exhibiting four yield stress values f_y=355, 460, 550 MPa (one has f_y=∞ for elastic columns).

Figure 7 shows the elastic and elastic-plastic equilibrium paths P/P_{cr} vs. v/t, describing the post-buckling behaviour of columns (i) containing initial imperfections defined by θ=0°, 15, 30, 45°, 60, 75, 90° and (ii) exhibiting yield stress values f_y=355, 460, 550MPa. Finally, Figure 8 provides information concerning the evolution of the plastic strains in the two columns defined by θ=0° and θ=90° – f_y=460MPa – in each case, one presents four plastic strains diagrams, corresponding to different equilibrium states located on the post-buckling path (their locations are indicated in Figure 8(a)).

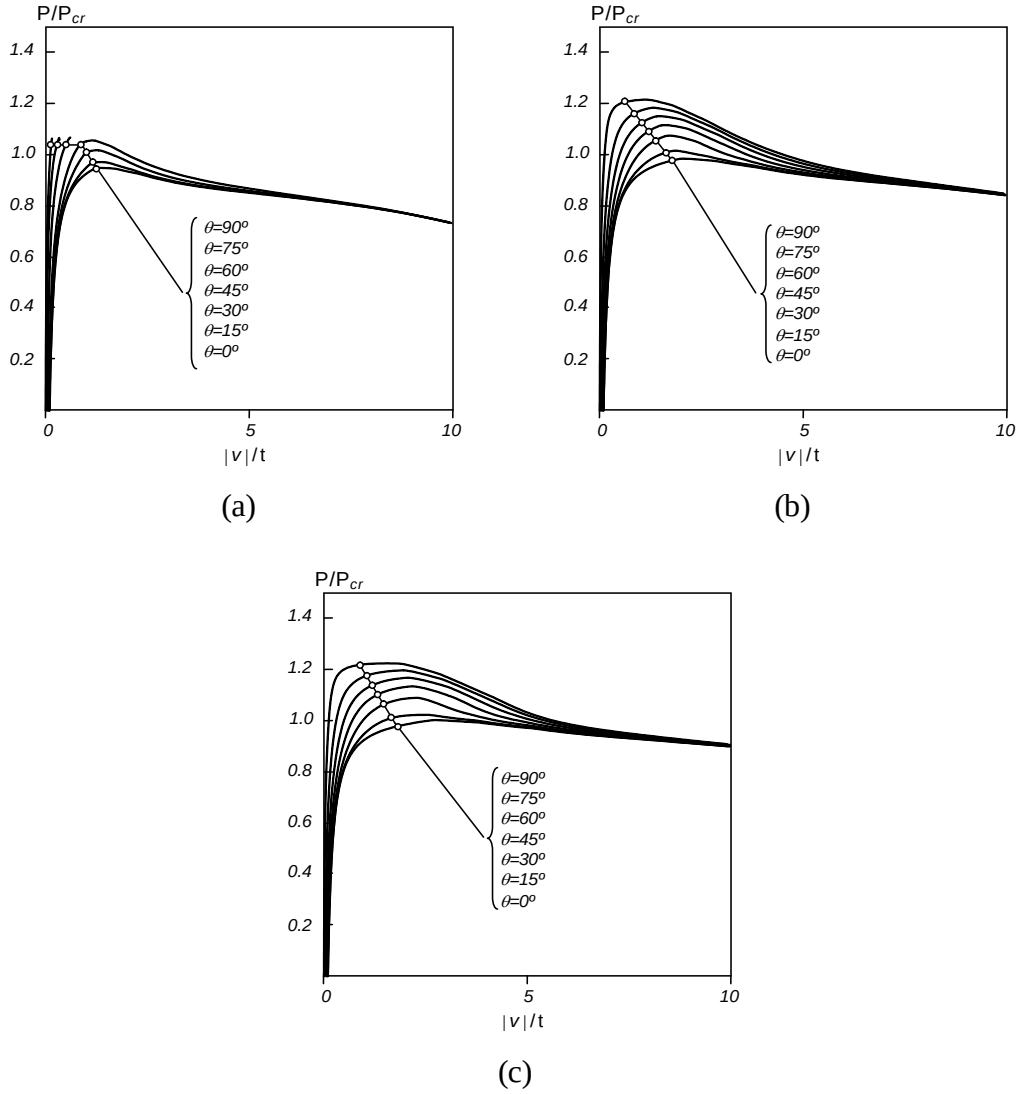

Figure 7. Column elastic and elastic-plastic (f_y=*355, 460, 550MPa*) post-buckling equilibrium paths

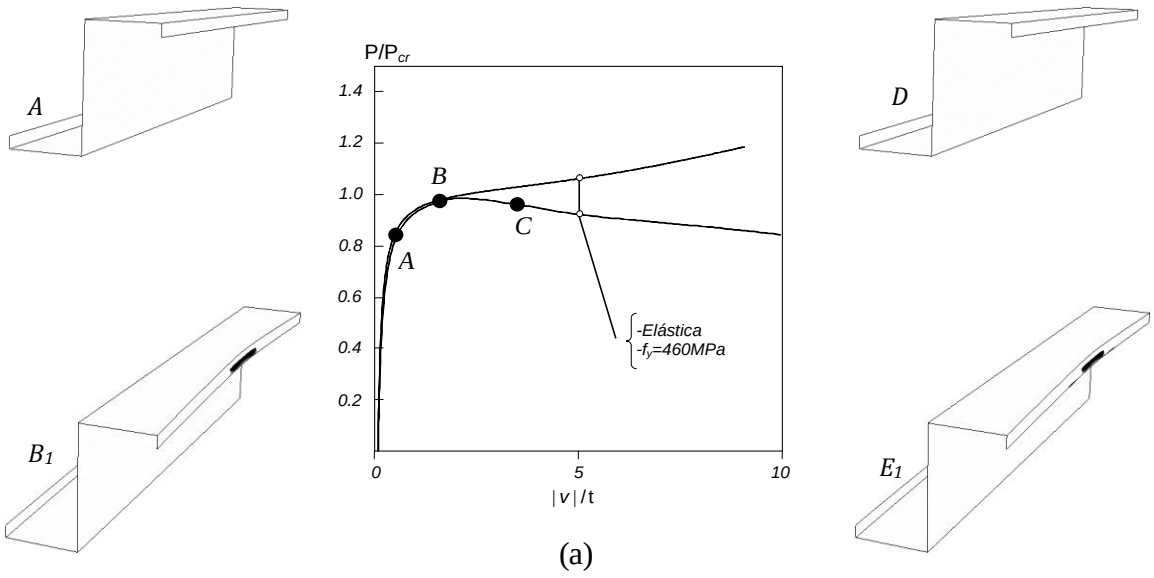

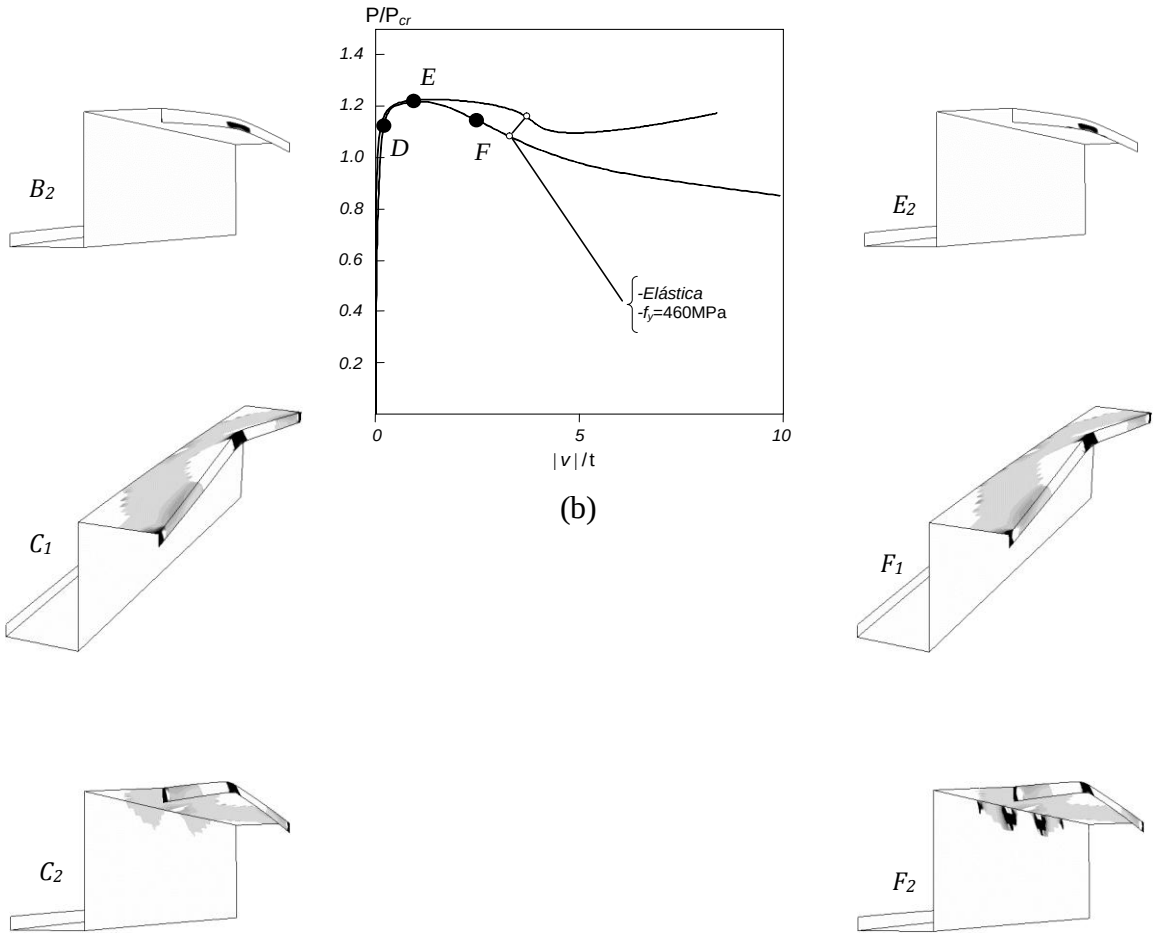

Figure 8. Elastic and elastic-plastic post-buckling equilibrium paths concerning the columns with pure (a) distortional (θ=0°) and (b) local-plate (θ=90°) initial imperfections. On the sides are represented the plastic strain diagrams and failure modes of the columns.

The observation of the post-buckling equilibrium paths and plastic strain diagrams displayed in the figures prompts the following remarks:

(i) Comparably to the elastic regime, it can be argued that the various elastic-plastic post-buckling trajectories eventually evolve similarly, with slight differences during evolution, but no significant differences with the column's ultimate strength.

(ii) The imperfections that lead to elastic-plastic post-buckling reduced resistance continue to be associated with pure distortional imperfections $\theta=0°$ (and by symmetry $\theta=180°$).

(iii) The columns that show greater resistance are associated with pure local imperfections $\theta=90°$ (and by symmetry $\theta=270°$).

5. Concluding Remarks

This work dealt with a numerical investigation concerning the elastic-plastic post-buckling behaviour of cold-formed steel Z-section columns, with extreme articulated sections, affected by local-plate/distortional buckling mode interaction. The analysis (i) involved columns containing several initial imperfections with similar combined amplitudes, obtained through different combinations of the competing buckling modes (5-wave local-plate and 1-wave distortional modes), and (ii) were performed using the finite element method (code ABAQUS and columns discretised be means of fine meshes of S4 shell elements). After addressing a number of relevant finite modelling issues, one presents and discussed several numerical results, which consisted of (i) elastic and elastic-plastic post-buckling equilibrium paths, (ii) curves describing the evolution of the column

deformed configurations along the elastic paths and (iii) figures providing information about the effect of the initial imperfection shape on the spread of plasticity and column elastic-plastic failure mode.

Among the various conclusions drawn from this investigation, the following ones deserve to be specially mentioned:

(i) The columns show some post-buckling elastic resistance and (i_1) evolve to deformed post-buckling configuration shapes that combine the distortional mode with 1-wave (predominant) and the local mode with 5-wave.

(ii) The post-buckling trajectories exhibit, in most cases, an irregular behaviour (e.g. limit points, instability by "snap-through") resulting from the column's adaptation to the final configuration (with local/distortional modes interaction).

(iii) The imperfections that lead to elastic-plastic post-buckling reduced resistance are those with pure distortional imperfections $\theta=0°$ (and by symmetry $\theta=180°$).

(iv) The columns show a significant elastic-plastic resistance, whose value increases with the steel yield strength and depends on the initial geometric imperfection.

6. References

[1] Schafer, B. (2008). Review: the direct strength method of cold-formed steel member design, Journal of Constructional Steel Research.

[2] Schafer, B. W., & Peköz, T. (1999). Laterally braced cold-formed steel members with edge-stiffened flanges, Journal of Structural Engineering (ASCE).

[3] Ungureanu, V., & Dubina, D. (2004). Recent research advances on ECBL approach – Part I: plastic-elastic interactive buckling of cold-formed steel sections, Thin-Walled Structures.

[4] Yang, D., & Hancock, G. (2004). Compression tests on high strength steel columns with interaction between local and distortional buckling, Journal of Structural Engineering (ASCE).

[5] Silvestre, N., & Camotim, D. (2002). GBT – Based Distortional Buckling Formulae for Thin-walled Channel Columns and Beams. Proceedings of 3th European Conference on Steel Structures (Eurosteel 2002), Coimbra.

[6] Dinis, P. B., & Camotim, D. (2005). Interacção local-de-placa/distorcional em colunas de aço enformadas a frio: análise por elementos finitos em regime elástico e elasto-plástico. Congresso de Métodos Numéricos en Ingeniería, Granada (4-7/7).

[7] Simulia Inc. (2008). ABAQUS Standard (version 6.7-5)

[8] Dinis, P. B., & Camotim, D. (2004). Local plate and distortional post-buckling behaviour of cold-formed steel columns: elastic and elastic-plastic FEM analysis. Proceedings of SSRC Annual Stability Conference, (Long Beach – 24-27/3).

[9] Dinis, P. B., & Camotim, D. (2003). Estabilidade de Perfis de Aço Enformados a Frio: Modelação por Elementos Finitos e Estudo da Influência das Condições de Apoio. VII Congresso de Mecânica Aplicada e Computacional, Universidade de Évora (14-16/4).

[10] Camotim, D., Silvestre, N., & Dinis, P.B. (2005). Numerical Analysis of Cold-formed Steel Members. International Journal of Steel Structures.

[11] Young, B., Camotim, D., & Silvestre, N. (2009). Ultimate strength and design of lipped channel columns experiencing local/distortional mode interaction – Part I: Experimental Investigation, Proceedings of Sixth International Conference on Advances in Steel Constructions, Hong Kong (December 2009), in press.